- Technical Paper -

SHEAR BEHAVIOR OF HIGH STRENGTH CONCRETE BEAMS

S.V.T. Janaka PERERA[*1], Hiroshi MUTSUYOSHI [*2], Ryosuke TAKEDA[*3], and Shingo ASAMOTO[*4]

ABSTRACT

High strength concrete (HSC) over 100 N/mm^2 beams have led to some concerns about their shear capacity because it produces high brittleness, smooth failure surface, and high early age shrinkage. In this study five HSC beams without shear reinforcement were tested. Test results indicated that the surface roughness of the specimen with concrete strength 138 N/mm^2 was 10% lower than the specimen with concrete strength 52 N/mm^2. Also the normalized shear strength of HSC beams was more dependent on the brittleness of the concrete than the roughness index, or the shrinkage.

Keywords: brittleness, concrete, roughness, shear strength, shrinkage

1. INTRODUCTION

High-strength concrete (HSC) is being increasingly used in buildings and bridges because it enables the use of smaller cross-sections, longer spans, reduction in girder height and improved durability [1]. Presently the target compressive strength of concrete easily exceeds 100 N/mm^2. However, the diagonal shear capacity of HSC beams does not increase as expected with the increase in the compressive strength of concrete [2]. Also, an increase in the concrete compressive strength produces an increase in its brittleness, smoothness of shear failure surface, and shrinkage due to self-desiccation at early ages. These limitations have led to some concerns about diagonal shear capacity of HSC beams.

The diagonal shear force in reinforced concrete (RC) members is transferred in various ways. After development of flexural cracks, shear force acting on a cracked section is carried by: 1) the shear resistance of un-cracked concrete in the compression zone; 2) the interlocking action of aggregates along the rough concrete surfaces on each side of the crack; and 3) the dowel action of the longitudinal reinforcement as shown in Fig.1. For rectangular beams, approximately 53-90% of the vertical shear is carried by aggregate interlocking and un-cracked concrete in the compression zone [3].

According to past studies the effect of HSC on shear transfer mechanism is as follows. The shear resistance of un-cracked concrete in the compression zone is reduced due to the brittleness of HSC [4]. The crack surface of HSC beams is relatively smoother than normal strength concrete (NSC) because cracks penetrate through aggregates. This smooth crack surface reduces the aggregate interlock and the shear strength of HSC beams [2]. Until now, little previous work has attempted to quantitatively evaluate the roughness of concrete fracture surfaces. Also, early age shrinkage causes deterioration in shear strength at diagonal cracking of reinforced HSC beams. Maruyama et al. [5] detected cracking around reinforcing bars due to early age shrinkage (autogenous shrinkage) of HSC, and from the comparison of self-induced stress in RC prisms with different early age shrinkages, concluded that this crack degrades bond stiffness. Therefore, the dowel action of the longitudinal reinforcement is affected by early age shrinkage. Most of above studies have been done for concrete with strength of less than 100 N/mm^2 due to design limitations [2].

Based on such a background, the objectives of this study are: 1) to explain effect of brittleness, failure surface roughness, and early age shrinkage on the shear behavior of HSC beams quantitatively; and 2) to determine the shear capacity of HSC beams using available prediction model. In this study concrete strengths of 120 and 160 N/mm^2 were used.

2. SHEAR CAPACITY PREDICTION

In order to get a high accuracy for shear capacity prediction the modified compression field theory (MCFT) was adopted in this study [6]. For ease of understanding the theory of MCFT is described using simplified MCFT [7].

The fundamental relationship in the simplified MCFT relates the shear stress, which can be transmitted across cracked concrete [7]. The equation is,

$$V_c = \beta f'_c{}^{0.5} b_w d_v \quad (1)$$

where, V_c: concrete contribution to shear strength (kN); f'_c: characteristic compressive strength of concrete (N/mm^2); d_v: the effective shear depth can be taken as $0.9d$, d is effective depth of the beam (mm); b_w: width of the beam (mm). The term β in Eq. (1) is a parameter

*1 Graduate Student, Graduate School of Science and Engineering, Saitama University, JCI Member
*2 Professor, Graduate School of Science and Engineering, Saitama University, JCI Member
*3 Graduate Student, Graduate School of Science and Engineering, Saitama University, JCI Member
*4 Asst. Professor, Graduate School of Science and Engineering, Saitama University, JCI Member

that models the ability of cracked concrete to transfer shear (see Eq. (2)). It is a function of: 1) the longitudinal strain at the mid-depth of the member ε_x (see Eq. (3)); 2) the crack spacing at the mid-depth (see Eq. (4)); and 3) the maximum coarse aggregate size a_g.

$$\beta = \frac{0.4}{(1 + 1500\varepsilon_x)} \cdot \frac{1300}{(1000 + s_{xe})} \quad (2)$$

The longitudinal strain at mid height ε_x is conservatively assumed to be equal to ½ the strain in the longitudinal tensile reinforcing steel. For sections that are not subjected to axial loads, ε_x is calculated as

$$\varepsilon_x = (M/d_v + V)/(2E_sA_s) \quad (3)$$

where, M: moment (kNmm); V: shear force (kN); E_s: Young's modulus of steel (kN/mm^2); A_s: area of longitudinal tensile steel (mm^2). To account for the effect of maximum aggregate size on shear behavior, an equivalent crack spacing factor s_{xe} (mm) is used.

$$s_{xe} = 35s_x/(16+a_g) \quad (4)$$

where, s_x can be taken as d_v [7].

Aggregate size does not influence aggregate interlock capacity in HSC because of smooth fracture surface. To account for this, it is suggested that an effective maximum aggregate size be calculated by linearly reducing a_g to zero as f'_c increases from 50 to 100 N/mm^2 [2]. In calculating Vc, the $f'^{0.5}_c$ is limited to a maximum of 8.3 N/mm^2 [8].

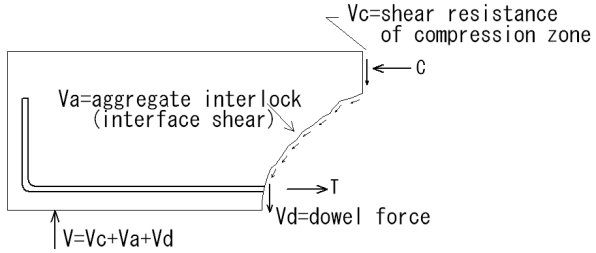

Figure 1: Shear transfer mechanism of slender beams

3. TEST PROGRAMS

3.1 Details of materials and specimens

The concrete mix proportions are tabulated in Table 1. The properties of aggregates and steel bars used in the experiment are listed in Tables 2 and 3.

As tabulated in Table 4, five identical beams without web reinforcement were used in this study. The cross sections and layout of test beams are shown in Fig. 2. Three high strength steel bars (f_y = 750 N/mm^2) were laid at the bottom of the section so shear failure would precede flexural failure. The test variables were compressive strength of concrete, early age shrinkage and aggregate type which are shown in Table 4. The shear span to effective depth (a/d) ratio was 4.0 for all beams.

All specimens including RC beams, compressive strength specimens (Φ100x200mm), splitting tensile strength specimens (Φ150x300mm), and fracture energy specimens (100x100x400mm) were cured up to the loading test age, to exclude the drying effects.

3.2 Instrumentation and measurements

(1) Beam test

The four point symmetrical loading with distance of 300 mm between the loading points was statically applied to all specimens (Fig.2). Vertical deflections at the center, shear span and support of the RC beam were measured by displacement transducers. Electrical-resistance strain gauges were used to record the strain in concrete at the mid span of the beam. All cracks, which developed during the loading were observed and marked in detail. The test was stopped when the crushing of the concrete in compression and considerable loss of load carrying capacity was observed.

(2) Early age shrinkage test

The early age shrinkage of concrete was started to measure just after concrete placement. A strain gauge was embedded at the middle height of the center of the prism (100x100x400mm, shown in Fig.3). The expansion/ shrinkage strain and the temperature of concrete were measured using the embedded gauge.

(3) Surface roughness index test

For surface roughness test, fractured splitting tensile strength test specimens were tested because it was used to measure tensile capacity of concrete. A laser light confocal microscope was used to scan the fractured surface three dimensionally (Fig. 4). A 100mmx100mm (at the center of the specimen) area of fractured surface was scanned with a 250μm pixel size and resolution of 0.01μm.

The compressive strength, splitting tensile strength, and fracture energy of concrete were measured according to Japanese Industrial Standard (JIS, 2005) on the same day as the RC beam test.

3.3 Roughness index of the fracture surface (R_s)

This section describes the process of fracture using important postmortem evidence, the fracture surface. It is commonly recognized that the roughness of the fracture surface of concrete can vary depending on mix design. HSC will often exhibit brittle behavior,

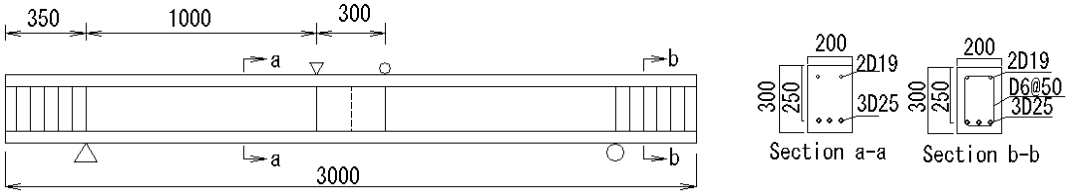

Figure 2: Details of RC beam (unit: mm)

Table 1: Mix proportions of concrete

Name of concrete	W/B (%)	Unit weight (kg/m^3)						
		W	SF	S	G	EX	SP	DA
HA120	20	155	775	703	792	-	11.63	0.78
LA120	20	155	750	703	792	25	11.63	0.78
HA160	17	155	912	592	792	-	14.59	0.91
HSA160	17	155	912	611	783	-	14.59	0.91
LA160	17	155	882	595	792	30	14.59	0.91

B= SF+EX
B: Binder, W: Water
SF: Silica fume cement, S: Sand
G: Gravel (maximum size of aggregate is 20mm)
EX: Expansive additive
SP: Super plasticizer
DA: Air reducing admixture

Table 2: Properties of aggregates

Type	Density (g/cm^3)	Absorption (%)	Fineness Modulus
A1	2.64	0.42	6.64
A2	2.54	2.74	6.57

Table 3: Mechanical properties of steel

Type	f_y (N/mm^2)	E_s (kN/mm^2)
D6	360	187
D19	384	200
D25	750	201

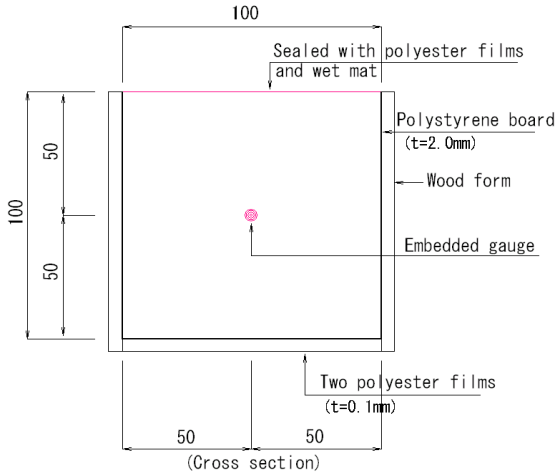

Figure 3: Details of early age shrinkage specimen (unit: mm); *t*: thickness

and cracks will propagate through the aggregate. In NSC, less brittle behavior is associated with tortuous fracture surfaces dominated by the size and distribution of aggregates. The roughness index (R_s) can be calculated by directly measured surface area (Fig. 5).

$$R_s = \frac{\text{actual surface area}}{\text{projected surface area}} = \frac{\Sigma Ai}{\Sigma \underline{A}} \quad (5)$$

To explain the effect of aggregate interlocking on shear capacity of HSC beams, the relationship between surface roughness and a_g (Eq. (4)) will be discussed later.

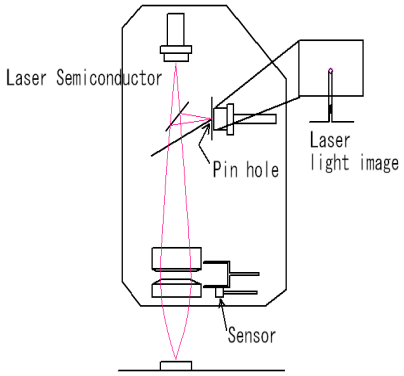

Figure 4: Schematic view of laser color confocal microscope computation

Table 4: Test variables

Specimen	f_c (N/mm^2)	Concrete shrinkage	Aggregate type
HA120	120	HA	A1
LA120	120	LA	A1
HA160	160	HA	A1
HSA160	160	HA	A2
LA160	160	LA	A1

f_c: Design compressive strength of concrete
A1: Granite, A2: Andesite
HA: High autogenous shrinkage
LA: Low autogenous shrinkage
HSA: High strength aggregate

3.4 Brittleness number (*B*)

Various parameters have been proposed to characterize the brittleness of concrete. The characteristic length, $l_{ch}=EG_F/f_t^2$, proposed by Hillerborg [9] has been used to characterize the brittleness of concrete, rock and glass. The normalized shear strength v_c/f'_t (v_c: shear strength) of geometrically similar beams, is governed by the dimensionless ratio between absolute structure size (D) and l_{ch} [10]. This ratio has been regarded as a measure of the brittleness of structural elements which sensitive to tensile stress induced fracture, a higher the value of B corresponding to a more brittle structural element.

$$B = f_t^2 D / (EG_F) \quad (6)$$

where; f_t: tensile strength (N/mm^2), E: Young's modulus (N/mm^2), G_F: fracture energy (N/mm), D: absolute structural element size (mm; in the case of a beam it is equal to effective depth of the beam). Tensile strength and modulus of elasticity of concrete are dependent on compressive strength, and fracture energy is dependent on aggregate size and compressive strength.

4. RESULTS AND DISCUSSION

4.1 Properties of concrete

The compressive strength, splitting tensile strength, Young's modulus, fracture energy and shrinkage strain in concrete at the age of beam test are tabulated in Table 5. The results show that the

compressive strength, splitting tensile strength, Young's modulus, fracture energy and shrinkage strain were 138-183 N/mm^2, 7.2-8.5 N/mm^2, 39.4-44.7 kN/mm^2, 0.195-0.280 N/mm, and (-114)-(-484) microns respectively. According to test results, a 15% increase in f'_t was observed in low autogenous (LA) concrete beams compared with high autogenous (HA) and high strength aggregate (HSA) concrete beams. But E_c and G_f of LA concrete beams were not significantly higher than HA and HSA concrete beams. In other words, the effect of early age shrinkage on mechanical properties of concrete was not noticeable other than f'_t.

4.2 Deformation of HSC beams

Fig. 6 shows the load-deflection response for tested beams. The explanation of the behavior of response curves is done with LA120 beam. In the LA120 response curve, flexural cracks first appeared at the early stage of loading. The load slightly dropped after the formation of the first flexural crack, and it continued to increase. Then, a diagonal crack occurred in the shear span and the load dropped sharply. However, soon after that, the load continued to increase, slightly dropping again with the formation of another crack. Even though diagonal cracking took place, the beam was still able to resist the applied load through arch action, as expected in HSC beams [2]. Finally beam failed in shear compression where the diagonal cracks in the shear span were widened and the concrete near the crack tip in the compression zone crushed. Beams LA120, HA160 and LA160 failed in shear compression and beams HA120 and HSA160 failed in diagonal tension. The diagonal tension failure occurred just after the critical diagonal cracking.

According to test results, flexural cracks were developed to a greater extent in HA beams (including HSA160 beam) than in LA beams before critical diagonal cracking. This was due to the shrinkage, as expected (Fig. 7) [11]. Also, those load-deflection relationships of all beams were similar up to diagonal cracking load.

LA beams tended to fail at higher loads in shear compression after forming an arch mechanism compared with HA beams. This behavior was mainly due the strength of compression strut and it is closely related to compressive strength of concrete. Also, reduced early age shrinkage in LA beams improved the bond stiffness of reinforcement and concrete [5].

Table 5: Outline of test results

Name of specimen	At the age of loading					V_c (kN)	V_u (kN)	Failure mode	R_s
	f'_c (N/mm^2)	f'_t (N/mm^2)	E_c (kN/mm^2)	G_f (N/mm)	ε_{sh} (x10^{-6})				
HA120	138	7.2	39.4	0.234	-412	165	165	DT	1.073
LA120	155	8.3	41.0	0.280	-114	170	241	SC	1.060
HA160	183	7.4	43.5	0.271	-454	150	211	SC	1.047
HSA160	164	7.6	44.2	0.195	-484	127	135	DT	1.076
LA160	175	8.5	44.7	0.259	-182	134	306	SC	1.056
S-40-3-4.0 [2]*	(52)	(4.2)	(32.1)	(0.200)	-	153	153	DT	(1.193)
S-100-3-4.0 [2]*	(114)	(6.2)	(42.9)	(0.220)	-	170	170	DT	-

f'_c: Compressive strength of concrete, f'_t: Splitting tensile strength of concrete, E_c: Young's modulus of concrete
G_f: Fracture energy, ε_{sh}: Shrinkage strain, V_c: Shear force at critical diagonal cracking, V_u: Shear force at failure
DT: Diagonal tension failure, SC: Shear compression failure, R_s: Surface roughness index
*: Beam details which are similar to Fig.2, ( ): Author's previously unpublished data

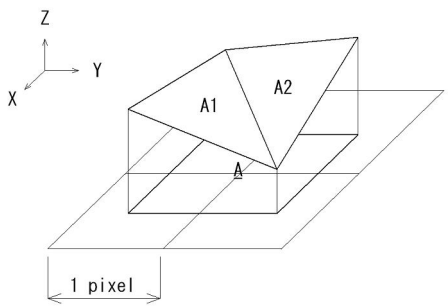

Figure 5: Schematic view of roughness parameter (R_s= Σ Ai/ Σ $\underline{A}$)

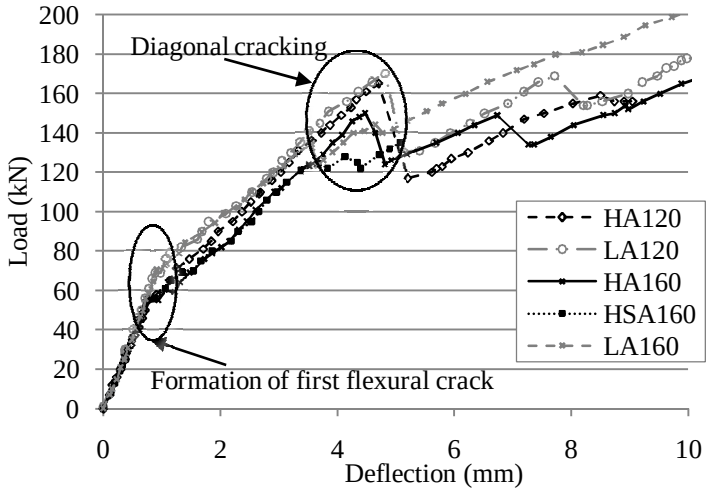

Figure 6: Comparison of load –deflection relationship of RC beams

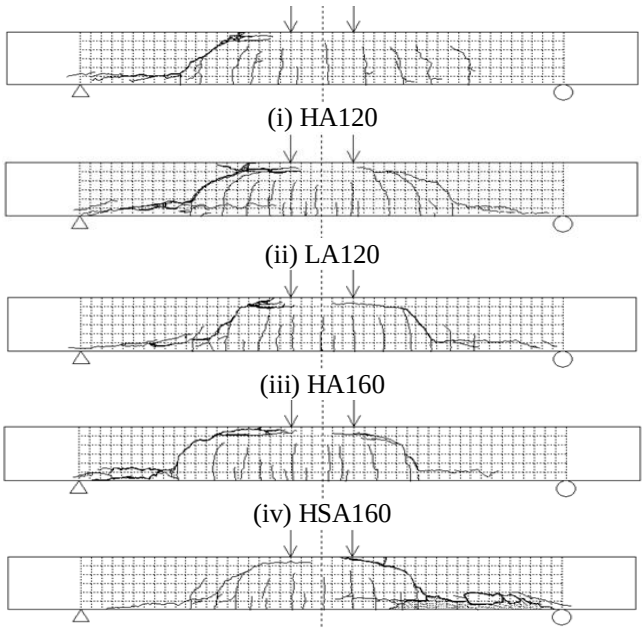

Figure 7: Beam crack pattern (just after failure)

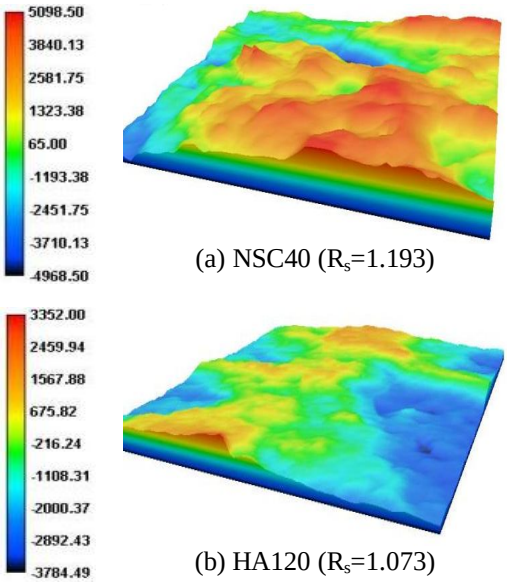

Figure 8: Fracture surface of splitting tensile strength test specimens (color code represent the surface elevation (μm))

4.3 Comparison of shear behavior of HSC beams

To analyze the brittleness and diagonal cracking load relationship in detail, the normalized shear strength (v_c/f'_t) was used (v_c: diagonal cracking strength). Brittleness (B) is inversely proportional to material shear strength. Therefore, for better understanding, $1/B$ was analyzed with v_c/f'_t.

According to Figures 8 and 9, the values of $1/B$ and R_s decreased by 52% and 10% with the increase of concrete strength, from NSC (52N/mm^2) to HSC (138 N/mm^2). The value of v_c/f'_t decreased from 0.73 to 0.33. In this region, the area of un-cracked compression zone of the beam also decreased with an increase in concrete strength. Because of high brittleness, this thin un-cracked compression zone was reduced further by flexural cracking. As a result of these factors the normalized shear carrying capacity of HA120 beam was reduced by 55%.

The surface roughness index did not significantly change when concrete strength changed from 138N/mm^2 to 175N/mm^2. Here, HSA160 beam had a 3% increase in R_s, but v_c/f'_t was lowest in this strength region due to corresponding lowest $1/B$ value from all beams. Also, the v_c/f'_t and $1/B$ were slightly reduced to 0.32 and 0.65 at concrete strength 175N/mm^2 respectively. In this concrete strength region normalized shear strengths of both LA120 and LA160 were lower than HA120 and HA160 beams respectively. This is because of the lower $1/B$ value in LA beams than HA beams (LA beams were more brittle).

At concrete strength 183N/mm^2, an increase in both v_c/f'_t (0.41, 28% increase) and $1/B$ (0.8, 25% increase) was seen. At the same time R_s decreased by 1% at concrete strength 183N/mm^2. Therefore, from Fig.9 it is possible to conclude that behavior of v_c/f'_t and $1/B$ of HSC beams was proportionate. Also, the normalized shear strength of HSC beams was more dependent on the brittleness of the concrete than the roughness index and the shrinkage.

To improve v_c/f'_t of HSC beams it is necessary to improve R_s or 1/B. The R_s value can be improved using high strength aggregates. As mentioned above, $1/B$ is a function of f'_t, E_c and G_F. Both f'_t and E_c are dependent on compressive strength of concrete, but G_F is mainly dependent on aggregate size and compressive strength. Therefore, to improve diagonal shear capacity of HSC beams it is necessary to improve both R_s and G_F by increasing compressive strength of aggregate.

5. PREDICTION OF SHEAR CAPACITY

According to Eq. (4), crack spacing decreases with the increase of a_g and then it improves the ability of cracked concrete to transfer shear. Therefore, in this study value of a_g was changed to represent the influence of fracture surface roughness. The surface roughness of NSC beam is 10% higher than HA120 beam. Therefore, during the analysis a_g was assumed as zero for all beams except NSC beam. For NSC (S-40-3-4.0) beam a_g = 20mm was used.

Table 6 shows the prediction results of diagonal cracking strength of RC beams. According to prediction results, except for the beams HSA160 and LA160, all other beams' shear predictions were within a margin of 10% error. The main reason for this error in predictions was most likely the brittleness of HSC. Because the value of $1/B$ was lower in both HSA160 and LA160 beams than other beams (Fig.9). Therefore, the MCFT should be modified to evaluate material brittleness and more testing is required in order to study this problem.

6. CONCLUSIONS

Conclusions may be summarized as follows;

(1) With LA concrete a 15% of increase in f'_t was achieved.

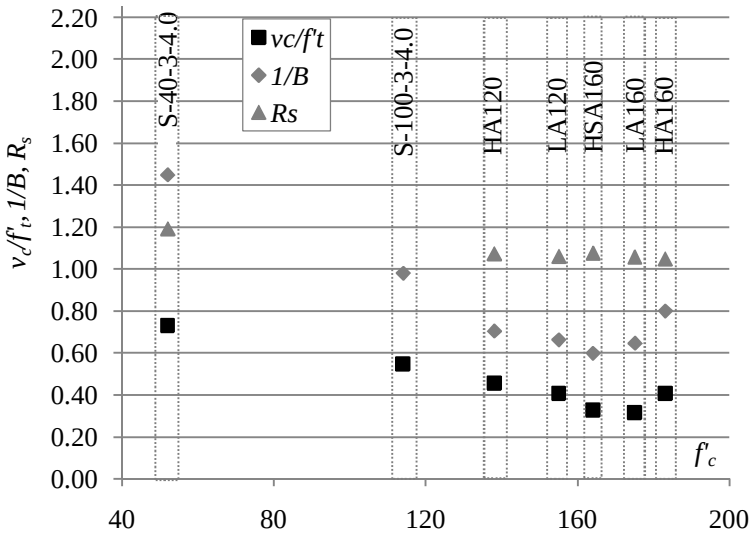

Figure 9: Test results comparison;
v_c/f'_t: normalized shear strength, 1/B: 1/Brittleness,
R_s: Roughness index

Table 6: Shear strength prediction

Specimen	v_c N/mm^2	v_{cal} N/mm^2	v_c/v_{cal}
HA120	1.65	1.67	0.99
LA120	1.70	1.82	0.93
HA160	1.50	1.59	0.94
HSA160	1.27	1.70	0.75
LA160	1.34	1.60	0.84
S-40-3-4.0 [2]	1.53	1.40	1.09
S-100-3-4.0 [2]	1.70	1.60	1.06

v_c: Shear strength at critical diagonal cracking,
v_{cal}: Predicted shear strength using MCFT [12]
$(a_g)_{HSC}$ = 0mm,
$(a_g)_{NSC}$ = 20mm

(2) The roughness index of specimens with a concrete strength 138 N/mm^2 is 10% lower than the specimen with concrete strength 52 N/mm^2.
(3) The normalized shear strength of HSC beams was more dependent on the brittleness of the concrete than the roughness index or the shrinkage.
(4) Diagonal shear capacity of HSC beams can be improved by improving R_S and G_F. Both R_S and G_F can be improved by increasing compressive strength of aggregates.
(5) The MCFT can predict the effect of the fracture surface roughness on diagonal shear strength capacity, but should be modified to predict the effect of brittleness of the concrete.

REFERENCES

[1] H. Mutsuyoshi, K. Ohtsuka, T. Ichinomiya, and M. Sakurada: Outline of Guidelines for Design and Construction of High Strength Concrete for Prestressed Concrete Structures, Proceedings of 8th International Symposium on Utilization of High Strength and High Performance Concrete, JSCE, pp.111-117, Oct. 2008

[2] S. V. T. J. Perera, L. H. Quang, H. Mutsuyoshi, and H. Minh: Shear Behavior of Reinforced Concrete Beams Using High-Strength Concrete, Proc. of Japan Concrete Institute (JCI), Vol. 31, No.2, pp.589-594, 2009

[3] R. Taylor, and R. S. Brown: The Effect of the Type of Aggregate on the Diagonal Cracking of Concrete Beams, Magazine of Concrete Research, July 1963

[4] R. Gettu, Z. P. Bazant, and M. E. Karr: Fracture Properties and Brittleness of High Strength Concrete, ACI Materials Journal, Vol. 87, No. 66, pp.608-618, Nov.-Dec. 1990

[5] I. Maruyama, S. Kameta, M. Suzuki, and R. Sato: Cracking of High Strength Concrete Around Deformed Reinforcing Bar Due to Shrinkage, Int. RILEM-JCI Seminar on Concrete Durability and Service Life Planning, edited by K. Kovler, RILEM Publications S. A. R. L., Ein-Bokek, Israel, pp.104-111, 2006

[6] F. J. Vecchio, and M. P. Collins: The Modified Compression Field Theory for Reinforced Concrete Elements Subjected to Shear, ACI Journal Proceedings, Vol. 83, No.2, pp.219-321, March-April 1986

[7] E. G. Sherwood, E. C. Bentz, and M. P. Collins: Effect of Aggregate Size on Beam-Shear Strength of Thick Slabs, ACI Structural Journal, Vol. 104, No.2, pp.180-190, March 2007

[8] D. Angelakos, E. C. Bentz, and M. P. Collins: Effect of Concrete Strength and Minimum Stirrups on Shear Strength of Large Members, ACI Structural Journal, Vol. 98, No. 3, pp.290-300, May-June 2001

[9] A. Hillerborg: Results of Three Comparative Test Series for Determining the Fracture Energy G_F of Concrete, Materials and Structures, Research and Testing (RILEM, Paris), Vol. 18, No.107, pp.407-413, Sept.-Oct. 1985

[10] P. J. Gustafsson, and A. Hillerborg: Sensitivity in Shear Strength of Longitudinal Reinforced Concrete Beams to Fracture Energy of Concrete, ACI Structural Journal, Vol. 85, No.30, pp.286-294, May-June 1988

[11] R. Sato, and H. Kawakane: A New Concept for the Early Age Shrinkage Effect on Diagonal Cracking Strength of Reinforced HSC Beams, J. of ACT, Vol. 6, No. 1, pp.45-67, Feb. 2008

[12] E.C. Bentz: Sectional Analysis of Reinforced Concrete Members, PhD dissertation, Dept. Civil Engineering, University of Toronto, Toronto, Canada, 2000